Inorg. Chem. **2008**, *47*, 10921−10934

Inorganic Chemistry
Article

Metal-to-Metal Electron-Transfer Emission in Cyanide-Bridged Chromium−Ruthenium Complexes: Effects of Configurational Mixing Between Ligand Field and Charge Transfer Excited States

Yuan-Jang Chen,[†,‡] Onduru S. Odongo,[†] Patrick G. McNamara,[†] Konrad T. Szacilowski,[†,§] and John F. Endicott*[,†]

Department of Chemistry, Wayne State University, Detroit, Michigan 48202, and Department of Chemistry, Fu Jen Catholic University, Taipei Hsien 24205, Taiwan, R.O.C.

Received June 17, 2008

Irradiations of the transition metal-to-transition metal charge transfer (MMCT) absorption bands of a series of cyanide-bridged chromium(III)−ruthenium(II) complexes at 77 K leads to near-infrared emission spectra of the corresponding chromium(II)−ruthenium(III) electron transfer excited states. The lifetimes of most of the MMCT excited states increase more than 10-fold when their am(m)ine ligands are perdueterated. These unique emissions have weak, low frequency vibronic sidebands that correspond to the small excited-state distortions in metal−ligand bonds that are characteristic of transition metal electron transfer involving only the non-bonding metal centered d-orbitals suggesting that the excited-state Cr(II) center has a triplet spin configuration. However, most of the electronically excited complexes probably have overall doublet spin multiplicity and exhibit an excitation energy dependent dual emission with the near in energy Cr(III)-centered and MMCT doublet excited states forming an unusual mixed valence pair.

Introduction

Emission is expected from an electron transfer system when the energy difference between reactants and products, $E_{eg}^{0\prime 0}$, is sufficiently greater than the nuclear reorganizational energy, λ_r,[1,2] and such electron transfer emissions are well documented for molecules with organic or metal donors (D) and organic acceptors (A).[3−15] While such electron transfer emission spectra can provide unique information about the molecular and environmental parameters that govern electron-transfer rates in the Marcus inverted region,[2,10,11,14,16,17] the related transition metal-to-transition metal electron transfer (MMCT) emission is extremely rare.[18,19]

Our search for emission from MMCT excited states was originally initiated as a result of the observation that irradiations of the MMCT absorption bands of some $[(L)M^{III}(CN^-)Ru^{II}(L')]$ complexes (M = Cr or Co; L, L′ = am(m)ine ligands) in ambient aqueous solutions resulted in

* To whom correspondence should be addressed. E-mail: jfe@chem.wayne.edu.
† Wayne State University.
‡ Fu Jen Catholic University.
§ Present address: Jagiellonian University, Faculty of Chemistry, Ingardena 3, 30−060 Kraków, Poland (e-mail: szacilow@chemia.uj.edu.pl).

(1) Marcus, R. A. *Annu. Rev. Phys. Chem.* **1964**, *15*, 155.
(2) Marcus, R. A. *J. Phys. Chem.* **1990**, *94*, 4963.
(3) Crosby, G. A. *Acc. Chem. Res.* **1975**, *8*, 231.
(4) Sutin, N. *Acc. Chem. Res.* **1982**, *15*, 275.
(5) Meyer, T. J. *Prog. Inorg. Chem.* **1983**, *30*, 389.
(6) Oevering, H.; Verhoeven, J. W.; Paddon-Row, M. N.; Warman, J. M. *Tetrahedron* **1989**, *45*, 4751.
(7) Gould, I. R.; Farid, S. *J. Am. Chem. Soc.* **1988**, *110*, 7883.
(8) Juris, A.; Balzani, V.; Barigelletti, F.; Compagna, S.; Belser, P. l.; von Zelewsky, A. *Coord. Chem. Rev.* **1988**, *84*, 85.
(9) Kalyanasundaram, K. *Photochemistry of Polypyridine and Porphyrin Complexes*; Academic Press: New York, 1992.
(10) Barbara, P. F.; Meyer, T. J.; Ratner, M. *J. Phys. Chem.* **1996**, *100*, 13148.
(11) Graff, D.; Claude, J. P.; Meyer, T. J. In *Electron Transfer Reactions: Inorganic, Organometallic and Biological Applications*; Isied, S. S., Ed.; American Chemical Society: Washington, DC, 1997; p 183.
(12) Endicott, J. F.; McNamara, P. G.; Buranda, T.; Macatangay, A. V. *Coord. Chem. Rev.* **2000**, *208*, 61.
(13) Andersson, A.-M.; Schmehl, R. H. In *Electron Transfer in Chemistry*; Balzani, V., Ed.; Wiley-VCH: Weinheim, Germany, 2001; Vol. *1*, p 312.
(14) Koeberg, M.; de Groot, M.; Verhoeven, J. W.; Lokan, N. R.; Shephard, M. J.; Padden-Row, M. N. *J. Phys. Chem. A* **2001**, *105*, 3417.
(15) Endicott, J. F.; Uddin, M. J. *Coord. Chem. Rev.* **2001**, *219−221*, 687.
(16) Matyushov, D. V.; Ladanyi, B. M. *J. Phys. Chem. B* **1998**, *102*, 5027.
(17) Gould, I. R.; Noukakis, D.; Gomez-Jahn, L.; Young, R. H.; Goodman, J. L.; Farid, S. *Chem. Phys.* **1993**, *176*, 439.
(18) Endicott, J. F. In *Electron Transfer in Chemistry*; Balzani, V., Ed.; Wiley-VCH: New York, 2001; Vol. *1*, p 238.
(19) Endicott, J. F.; Chen, Y.-J.; Xie, P. *Coord. Chem. Rev.* **2005**, *249*, 343.

10.1021/ic8011266 CCC: $40.75
Published on Web 11/01/2008

transient electron transfer excited states that regenerated their ground states within a few nanoseconds,[20,21]

$$[(L)M^{III}(CN^{-})Ru^{II}(L')] + h\nu_{abs} \rightarrow [(L)M^{II}(CN^{-})Ru^{III}(L')]_{FC} \quad (1)$$

$$[(L)M^{II}(CN^{-})Ru^{III}(L')]_{FC} \rightarrow [(L)M^{II}(CN^{-})Ru^{III}(L')]_{VEq} + \Delta E_{eg} \quad (2)$$

where the subscripts "FC" and "VEq" designate the

$$[(L)M^{II}(CN^{-})Ru^{III}(L')]_{VEq} \rightarrow \begin{cases} [(L)M^{III}(CN^{-})Ru^{II}(L')] + h\nu_{em} \\ [(L)M^{III}(CN^{-})Ru^{II}(L')] + h\nu_{hf}\ (k_{et}) \end{cases} \quad (3)$$

"Franck−Condon" and "vibrationally equilibrated" excited states whose energies are E_{eg}^{FC} and $E_{eg}^{0'0}$, respectively, and $\Delta E_{eg} = (E_{eg}^{FC} - E_{eg}^{0'0})$. In these systems $E_{eg}^{0'0} \gg \lambda_r$ so that the back electron transfer to regenerate the ground states is in the Marcus inverted region, and complexes with such long ambient lifetimes are expected to give rise to luminesce at low temperatures. This was confirmed relatively recently and such electron transfer emission involving simple transition metal complex electron transfer couples has so far only been reported for Ru^{II} donor and Cr^{III} acceptor complexes which are linked by means of a cyanide ligand.[12,22,23] The present report describes our systematic studies of the 77 K luminescence in this class of D/A complexes.

The molecular parameters that govern the rates of electron-transfer processes (k_{et}) when $|E_{eg}^{0'0}| > \lambda_r$ are well-known to depend on a combination of electronic (typically represented in terms of an electronic matrix element, H_{DA}) and nuclear factors.[1,24] The latter include contributions from those differences in the molecular geometries and solvation of the reactants and products that contribute to λ_r;[1,2,10,24−26] furthermore, the electron transfer rate constant, k_{et}, in this regime is a function of the efficiency of depositing the excess energy in vibrational motions ($h\nu_{hf}$) and this depends on the overlap between the excited (or reactant) and ground-state vibrational wave functions where the latter involve high frequency vibrational modes with $h\nu_{hf} \sim E_{eg}^{0'0}$.[24] The $h\nu_{hf}$ that are large enough to meet these conditions correspond to the higher harmonics and combinations of the first order normal vibrational modes of the ground state whose equilibrium coordinates differ in the two electronic states.[10,17,24,27,28] However, the molecular distortions and identities of the first order vibrational modes that contribute to $h\nu_{hf}$ are very difficult to determine for very high energy reactant species, and even if the identities of the distortion modes were known, it is rarely clear how much they affect electron-transfer rates in the Marcus inverted region. These problems arise, in part, because (a) the distortion modes whose quanta are too large to be significantly populated thermally (modes for which $h\nu_h > \sim 4k_BT$) tend to be more important in determining k_{et} than the thermally populated low frequency vibrational modes ($h\nu_l \leq \sim 4k_BT$) that dominate electron transfer reactivity when $|E_{eg}^{0'0}| < \lambda_r$;[24] (b) the electronic excited states are often distorted in many different vibrational modes;[29−33] (c) most of the relevant systems involve covalently linked complexes in which the vibrational modes of the linking moieties may also play a role in determining the electron-transfer rates;[29,34] and (d) transition metal complexes typically have a large number of near in energy electronic excited states[19,35−38] and configurational mixing among them can alter excited-state structures and reactivity. Thus, in the systems of interest in this report, the stretching frequency of the bridging CN^- ligand is strongly correlated with the magnitude of the Ru^{II}/M^{III} MMCT electronic coupling in $[(L)M^{III}(CN^{-})Ru^{II}(L')]$ complexes (M = Cr, Co, and Rh) and the M^{III}-centered (*dd*) electronic transitions of these complexes are in approximately the same spectral region as their MMCT absorptions.[39−42] The Ru^{II}/M^{III} MMCT absorption bands are generally in the visible region (M = Rh is the exception) and they are especially intense for the M = Cr complexes (absorptivities $\sim 4 \times 10^3\ M^{-1}\ cm^{-1}$/Ru and $H_{DA} \sim 3 \times 10^3\ cm^{-1}$),[41,42] similar to the large values of H_{DA} that are characteristic of many covalently linked mixed valence Ru^{III}/Ru^{II} complexes.[39,43,44] Thus, the combination of configurational mixing with different, near in energy electronic excited states[19,35−38] and the large distortions of the MMCT excited states in relatively low frequency, metal−ligand vibrational modes that are characteristic of transition metal electron transfer, can make it especially difficult to understand the reactivity patterns of inverted region, transition metal-to-

(20) Endicott, J. F.; Song, X.; Watzky, M. A.; Buranda, T. *J. Photochem. Photobiol. A: Chem.* **1994**, *82*, 181.
(21) Endicott, J. F.; Watzky, M. A.; Macatangay, A. V.; Mazzetto, S. E.; Song, X.; Buranda, T. In *Electron and Ion Transfer in Condensed Media*; Kornyshev, A. A., Tosi, M., Ulstrup, J., Eds.; World Scientific: Singapore, 1997; p 139.
(22) Chen, Y.-J.; McNamara, P. G.; Endicott, J. F. *J. Phys. Chem.* **2007**, *111*, 6748.
(23) Chen, Y.-J.; Xie, P.; Endicott, J. F. *J. Phys. Chem. A* **2004**, *108*, 5041.
(24) Englman, R.; Jortner, J. *Mol. Phys.* **1970**, *18*, 145.
(25) Marcus, R. A. *Discuss. Faraday Soc.* **1960**, *29*, 21.
(26) Marcus, R. A. *J. Chem. Phys.* **1965**, *43*, 670.
(27) Freed, K. F.; Jortner, J. *J. Chem. Phys.* **1970**, *52*, 6272.
(28) Kestner, N.; Logan, J.; Jortner, J. *J. Phys. Chem.* **1974**, *64*, 2148.
(29) Hupp, J. T. In *Comprehensive Coordination Chemistry II*; McCleverty, J., Meyer, T. J., Eds.; Pergamon: Oxford, U.K., 2003; Vol. *2*, p 709.
(30) Hupp, J. T.; Williams, R. T. *Acc. Chem. Res.* **2001**, *34*, 808.
(31) Pertrov, V.; Hupp, J. T.; Mottley, C.; Mann, L. C. *J. Am. Chem. Soc.* **1994**, *116*, 2171.
(32) Maruszewski, K.; Bajdor, K.; Strommen, D. P.; Kincaid, J. R. *J. Phys. Chem.* **1995**, *99*, 6286.
(33) Thompson, D. G.; Schoonover, J. R.; Timpson, C. J.; Meyer, T. J. *J. Phys. Chem. A* **2003**, *107*, 10250.
(34) Ondrechen, M. J.; Gozashiti, S.; Zhang, L.-T.; Zhou, F. In *Electron Transfer in Biology and the Solid State*; Johnson, M. K., King, R. B., Kurz, D. M., Kutal, C., Norton, M. L., Scott, R. A., Eds.; American Chemical Society: Washington, DC, 1990;Vol. *226*, p 225.
(35) Seneviratne, D. S.; Uddin, M. J.; Swayambunathan, V.; Schlegel, H. B.; Endicott, J. F. *Inorg. Chem.* **2002**, *41*, 1502.
(36) Endicott, J. F.; Schegel, H. B.; Uddin, M. J.; Seneviratne, D. *Coord. Chem. Rev.* **2002**, *229*, 95.
(37) Alary, F.; Heully, J.-L.; Bijeireand, L.; Vicendo, P. *Inorg. Chem.* **2007**, *46*, 3154.
(38) Bolvin, H. *Inorg. Chem.* **2007**, *46*, 417.
(39) Endicott, J. F. In *Comprehensive Coordination Chemistry II*, 2nd ed.; McCleverty, J., Meyer, T. J., Eds.; Pergamon: Oxford, U.K., 2003; Vol. *7*, p 657.
(40) Macatangay, A. V.; Endicott, J. F. *Inorg. Chem.* **2000**, *39*, 437.
(41) Watzky, M. A.; Endicott, J. F.; Song, X.; Lei, Y.; Macatangay, A. V. *Inorg. Chem.* **1996**, *35*, 3463.
(42) Watzky, M. A.; Macatangay, A. V.; Van Camp, R. A.; Mazzetto, S. E.; Song, X.; Endicott, J. F.; Buranda, T. *J. Phys. Chem.* **1997**, *101*, 8441.
(43) Creutz, C. *Prog. Inorg. Chem.* **1983**, *30*, 1.
(44) Crutchley, R. *Adv. Inorg. Chem.* **1994**, *41*, 273.

transition metal electron transfer.[22,45−48] Furthermore, strong D/A electronic coupling can also lead to appreciable configurational mixing between the ground state and the lowest energy excited states to attenuate the extent of excited-state distortion.[19,35,36,47−49] Since variations in configurational mixing between near in energy electronic excited states can introduce molecular distortions that are not expected in the unmixed (or diabatic) states and/or attenuate the expected distortions,[45−47,50] both the energies and the shapes of the reactant and product potential energy (PE) surfaces can be difficult to predict from simple models.[19,47,50] The relevant differences in ground and excited-state molecular structures are manifested in differences in emission bandshapes, and we have explored some of these issues in this study of the 77 K MMCT emission spectra of $[(L)Cr^{III}(CN^-)Ru^{II}(L')]$ complexes.

The energies of the *dd* and MMCT excited states of the $[(L)Cr^{III}(CN^-)Ru^{II}(L')]$ complexes are very similar, and the lowest energy, ^{2}Cr(III) excited state of the Cr(III) complexes (the left superscript designates the doublet spin multiplicity, D), is typically in the range of $E_{Dg}^{0} \cong 13{,}000-15000$ cm^{-1}.[51,52] Since this is not much different from emission energies expected (e.g., based on $\Delta E_{eg} \sim 6{,}000$ cm^{-1} for $[Ru(Am)_{6-2n}(bpy)_n]^{2+}$ complexes where Am = an am(m)ine)[46,48] and found for the $[(L)Cr^{III}(CN^-)Ru^{II}(L')]$ complexes,[12,22,23] *dd*/MMCT configurational mixing could be an important feature in the excited-state properties of these complexes. Thus, the *dd* and CT electronic excited states are sufficiently different in molecular structure that the emission spectrum may contain features that are characteristic of each of the diabatic electronic configurations. For example, the distortions in metal−ligand vibrational modes that are observed in the MLCT excited-state emission spectra of $[Ru(Am)_{6-2n}(bpy)_n]^{2+}$ complexes has been attributed to such excited state/excited state configurational mixing.[46,50] When the *dd* and CT excited states are very similar in energy but only weakly mixed, the lowest energy adiabatic excited state may have local PE minima, analogous to those of ground state mixed valence complexes,[43,44,53,54] with structural characteristics that are only slightly changed from those of their diabatic analogues (see Figure 1), and such features have been observed in the emission spectrum of the *trans*-[(*ms*-Me_6[14]aneN_6)Cr({CN-$Ru(NH_3)_5$}$_2$]$^{5+}$ complex (*rac*-Me_6[14]aneN_6 a tetraaza-macrocyclic ligand; see Figure 2 below).[22] It is important to observe that the electronic structures in this series of complexes are far more complicated than implied by Figure 1, and this point is developed further below.

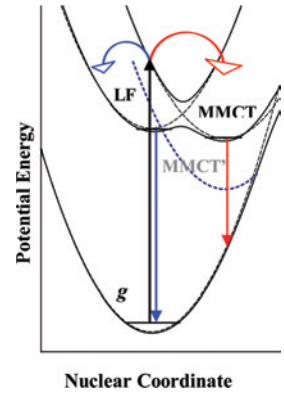

Figure 1. Qualitative PE curves illustrating the effects of configurational mixing between ligand field and MMCT excited states. The dashed PE curves represent the diabatic (unmixed) states and the solid curves the adiabatic electronic states. The vertical black arrow represents absorption and the vertical red and blue arrows represent emission. The red and blue arrows illustrate the possibility of a dual emission in a Cr(CN)Ru complex when the electronic coupling is weak and the lowest energy adiabatic PE surface has a double minimum. The MMCT′ diabatic PE curve illustrates the situation when the two excited states differ a great deal in energy and would result in a single adiabatic minimum and only emission characteristic of the MMCT′ component.

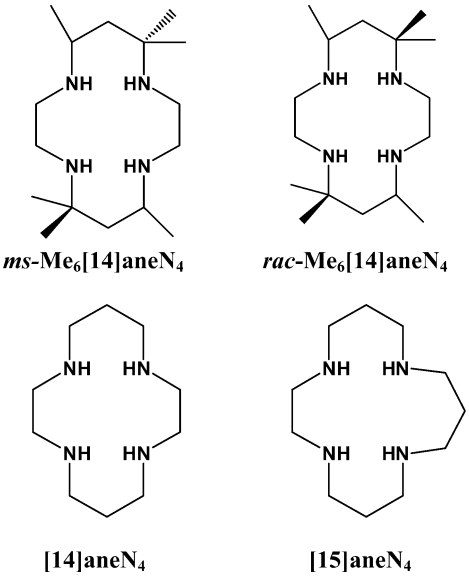

Figure 2. Skeletal structures of some macrocyclic amine ligands.

Experimental Section

A. Materials and Complexes. The ligands [14]aneN$_4$ (1,4,8,11-tetraazacyclotetradecane or cyclam), *ms*-Me$_6$[14]aneN$_4$ (5,12-*meso*-5,7,7,12,14,14-hexamethyl-1,4,8,11-tetraazacyclotetradecane or teta) and *rac*-Me$_6$[14]aneN$_4$ (5,12-*rac*-5,7,7,12,14,14-hexamethyl-1,4,8,11-tetraazacyclotetradecane or tetb) were synthesized according to literature procedures.[55,56] The [15]aneN$_4$ (1,4,8,12-tetraazacyclopentadecane) and bpy (2,2′-bipyridine) ligands were purchased from Aldrich. Figure 2 shows the skeletal structures of the macrocyclic amine ligands.

(45) Chen, Y.-J.; Xie, P.; Endicott, J. F.; Odongo, O. S. *J. Phys. Chem. A* **2006**, *110*, 7970.
(46) Chen, Y.-J.; Xie, P.; Heeg, M. J.; Endicott, J. F. *Inorg. Chem.* **2006**, *45*, 6282.
(47) Endicott, J. F.; Chen, Y.-J. *Coord. Chem. Rev.* **2007**, *251*, 328.
(48) Xie, P.; Chen, Y.-J.; Uddin, M. J.; Endicott, J. F. *J. Phys. Chem. A* **2005**, *109*, 4671.
(49) Endicott, J. F.; Uddin, M. J.; Schlegel, H. B. *Res. Chem. Intermed.* **2002**, *28*, 761.
(50) Odongo, O. S.; Heeg, M. J.; Chen, J. Y.; Xie, P.; Endicott, J. F. *Inorg. Chem.* **2008**, *47*, 7493.
(51) Forster, L. S. *Chem. Rev.* **1990**, *90*, 331.
(52) Endicott, J. F.; Ramasami, T.; Tamilarasan, R.; Lessard, R. B.; Ryu, C. K.; Brubaker, G. B. *Coord. Chem. Rev.* **1987**, *77*, 1.
(53) Hush, N. S. *Prog. Inorg. Chem.* **1967**, *8*, 391.
(54) Hush, N. S. In *Mechanistic Aspects of Inorganic Reactions*; Rorabacher, D. B., Endicott, J. F., Eds.; ACS Symposium Series 198; American Chemical Society: Washington, DC, 1982; p 301.
(55) Barefied, E. K.; Freeman, G. *Inorg. Synth.* **1980**, *20*, 108.
(56) Hay, R. W.; Lawrence, G. A.; Curtis, N. F. *J. Chem. Soc., Perkin Trans.* **1975**, 591.

Table 1. Half-Wave Potentials of $[(L)Cr^{III}(CN^-)Ru^{II}(L')]$ Complexes[a]

complexes	$E_{1/2}(Ru^{III/II})$, V, (ΔE_p in mV)	$E_{1/2}(Cr^{III/II})$ (ΔE_p in mV)[b]	$E_{1/2}(bpy^{0/-1})$ (ΔE_p in mV)[b]
$[Cr(NH_3)_5\{CNRu(NH_3\}_5)]^{4+}$	0.372 (69)[b]		
trans-$[Ru(NH_3)_4\{NC\text{-}Cr(NH)_5\}_2]^{6+}$	0.600 (80)[b]		
trans-$[Cr([14]aneN_4)\{CNRu(NH_3)_5\}_2]^{5+}$	0.321 (120)[c]		
trans-$[Cr(ms\text{-}(5,12)\text{-}Me_6[14]aneN_4)\ \{CNRu(NH_3)_5\}_2]^{5+}$	0.364 (121)[c]		
cis-$[Cr(rac\text{-}(5,12)\text{-}Me_6[14]aneN_4)\ \{CNRu(NH_3)_5\}_2]^{5+}$	0.320 (120)[d]		
cis-$[Cr(bpy)_2\{CNRu(NH_3)_5\}_2]^{5+}$	0.308 (110)[e]		
	0.229 (120), 0.351 (110)[f]	−0.541(120)[f]	−1.057(180)[f]
cis-$[Cr(bpy)_2(CN)_2]^+$		−0.515(120)[b]	−1.100(150)[b]

[a] In 0.1 M TEAP/CH_3CN with a Pt disk electrode and Internal ferrocene reference (0.367 V vs SSCE) except as indicated. [b] This work; scan rate = 200mV/s. [c] Watzky et al.[40] [d] Macatangay et al.[40] [e] Watzky, M. A., Ph. D. Dissertation, Wayne State University, 1994. [f] In 0.1 M TBAP/DMF. Pt disk electrode. Ferrocene (0.536 V vs Ag/AgCl). Scan rate = 500 mV/s.

The parent $[Cr(Am)_{6-n}(CN)_n]^{3-n}$ complexes were synthesized according to literature procedures.[57−61] The synthesis and characterization of most of the $[Cr^{III}CNRu^{II}]$ complexes has been described elsewhere.[41,42,62,63]

***trans*-[Ru(NH$_3$)$_4${NCCr(NH$_3$)$_5$}$_2$](PF$_6$)$_6$.** Solutions of *trans*-$[Ru(NH_3)_4(H_2O)_2](PF_6)_2$[64] (100 mg; 0.2 mmole) and $[Cr(NH_3)_5(CN)](PF_6)_2$ (183 mg; 0.4 mmole) in 20 mL of Ar purged acetone were kept at 40 °C in a reduced light dark box. After 4 days, the acetone solution was cooled and mixed with 100 mL of ether in an ice bath. The dark precipitate was separated by filtration, the filtrate was mixed with a solution of 5 mL of acetone and 5 mL of 50% saturated NH_4PF_6(aq), and the *trans*-$[Ru(NH_3)_4(NCCr(NH_3)_5)_2](PF_6)_6$ solid was obtained after several days by refrigeration. This yielded 150 mg (0.11 mmole) of product. Elemental analysis (C/H/N): 1.76:3.10:16.41 (calc), 1.72:3.16:16.30 (obsd).

B. Sample Preparation. The low temperature emission studies were performed using a 1:1 DMSO/water (V/V) mixture or butyronitrile as the solvent. Protio samples were dissolved in the solvent and loaded into a cylindrical (3 mm I.D.), Suprasil luminescence cell. The cell was then inserted into a spectroscopic Dewar flask and frozen with liquid nitrogen. Deuteration of the am(m)ine moieties in the complexes was performed in an argon atmosphere in a glovebag. The complexes were first dissolved in 99.9% pure deuterium oxide from Cambridge Isotope Laboratories, Inc. After mildly agitating for 10 min, an excess of $NaPF_6$ was added. The precipitate was collected after 30 min by vacuum filtration; this process was repeated two times. The deuterated precipitate was then dissolved in DMSO/D_2O (v/v 1:1) into 1 cm quartz cell. After mixing, 0.5 mL of this sample was removed and placed into a cylindrical (3 mm I.D.), Suprasil luminescence cell; the remaining sample was used to determine the UV−vis absorption spectrum. Spectroscopic grade dimethylsulfoxide (DMSO) was purchased from Fisher Scientific and used as supplied.

C. Instrumental Procedures. 1. Complex Characterization. The absorption spectra of most of these complexes have been reported previously.[20,41,42,62] UV−visible spectra were recorded for each complex used in this study using a Shimadzu UV-2101PC spectrophotometer; ^1H and ^{13}C NMR spectra were obtained using a Varian 300 MHz instrument.

Cyclic voltammograms (CV) were obtained in dry CH_3CN using a three-electrode system consisting of a Ag/AgCl reference electrode, a Pt wire counter electrode, and a Pt disk working electrode with a BAS model 100A electrochemical workstation for measurements. The solutions consisted of the complex dissolved in acetonitrile containing 0.1 mol/L tetrabutylammonium hexafluorophosphate as electrolyte. Ferrocene was dissolved in the sample solutions as an internal reference for the cyclic voltammograms. The electrochemical observations are summarized in Table 1.

2. Emission spectra. We have used three different instruments for the 77 K emission spectra of these complexes. The initial luminescence spectra were obtained by directing the radiation emitted from the sample by means of a fiber-optic into an Acton Research Corp. Spectra-Pro 500 spectrograph and dispersed onto a Princeton Instruments IRY-512 diode array. A Molectron UV-1010 nitrogen laser-pumped DL II/14 dye laser provided the excitation pulses for these measurements and was synchronized with the diode array in a modification of procedures described previously.[12,60,65] Typically, 300 shots were accumulated for each spectrum. The accumulated spectra were exported to Microsoft Excel and averaged. The wavelength response of the diode array was calibrated with the line emissions from a neon lamp. The raw sample spectrum was baseline corrected for dark current noise. Because the emissions were in a wavelength region in which diode array had limited sensitivity (the detector response was negligible at wavelengths greater than 900 nm), the resulting spectra were poorly resolved and the bandshapes were not well defined.[12] We also examined the emission spectra of the *trans*-$[(ms\text{-}Me_6[14]aneN_4)Cr\{CNRu(NH_3)_5\}_2]^{5+}$ complex using a commercial SPEX Tau2 fluorimeter. This fluorimeter has a wavelength range comparable to that of the IRY-512 diode array. Furthermore, the emission spectra of the Cr(CN)Ru complexes are excitation wavelength dependent[12,22,23] and the excitation in the Tau2 is not rigorously monochromatic, so that the emission bandwidths of the resulting spectra were significantly larger but otherwise in reasonably good agreement with those obtained with the OMA V.

The use of a PI OMA V InGaAs array detector (512 pixels) from Princeton Instruments (Roper Scientific) in combination with laser diode excitation, described previously[22,23,48,50] and below, has resulted in far better spectra. This detector was calibrated for wavelength using Xe emission lines, and for intensity using an Oriel model 63358 Quartz Tungsten Halogen QTH lamp. Emission spectra were obtained in 77 K glasses with the OMA V detector mounted on the Acton SP500 spectrometer equipped with a 300 g/mm grating, blazed at 1000 nm, as described in detail elsewhere.[23,48] The sample cell, Dewar and diode laser module used

(57) Riccieri, P.; Zinato, E. *Inorg. Chem.* **1980**, *19*, 853.
(58) Kane-Maguire, N. A. P.; Bennett, J. A.; Miller, P. K. *Inorg. Chim. Acta* **1983**, *76*, L123.
(59) Kane-Maguire, N. A. P.; Cripeen, W. S.; Miller, P. K. *Inorg. Chem.* **1983**, *22*, 696.
(60) Lessard, R. B.; Heeg, M. J.; Buranda, T.; Perkovic, M. W.; Schwarz, C. L.; Rudong, Y.; Endicott, J. F. *Inorg. Chem.* **1992**, *31*, 3091.
(61) Ryu, C. K.; Endicott, J. F. *Inorg. Chem.* **1988**, *27*, 2203.
(62) Endicott, J. F.; Song, X.; Watzky, M. A.; Buranda, T. *Chem. Phys.* **1993**, *176*, 427.
(63) Macatangay, A. V.; Mazzetto, S. E.; Endicott, J. F. *Inorg. Chem.* **1999**, *38*, 5091.
(64) Krentzien, H. J. Ph.D. Dissertation, Stanford University, 1976.
(65) Perkovic, M. W.; Heeg, M. J.; Endicott, J. F. *Inorg. Chem.* **1991**, *30*, 3140.

for excitation were aligned for each experiment to optimize the signal. Optical filters were used to reduce the scattered laser light. The effective observation window of the OMA V/SP500 instrument was 150 nm, and emission data were collected using the WinSpec program in the scan-accumulate-paste mode. Complexes were irradiated in their MMCT absorption bands using CW excitation provided by the diode laser modules: (a) MGL-S-B 50mW 532 nm (Changchun Industries Optoelectronics Tech Co. Ltd.) purchased from OnPoint Lasers, Inc.; (b) Power Technology, Inc. 405 nm 50 mW; and (c) Newport LPM658-65E 658 nm 65 mW. ASCII files were transferred to EXCEL and 10−30 spectra were averaged for each complex. For some experiments the higher energy CW excitation was provided by a model 1907 450W xenon lamp (model 1909 lamp housing and model 1907P power supply) with the model 1680 double-grating Spectramate monochromator (SPEX Industries. Inc.). The bandwidth range of this excitation light source was less than 5 nm (determined using the SP500/InGaAs array spectrometer).

The sample cells for lifetime determinations were placed in the spectroscopic liquid nitrogen filled Dewar. Monochromatic pulsed excitation was provided either by the Molectron UV1010 system used previously[48] or by a PRA LN 1000 nitrogen laser with a LN 107 dye laser. The radiation emitted at 90° to the excitation beam was approximately focused into a J/Y H-100 spectrometer connected to a Hammamatsu 955R PMT. Because signal intensities were small, the H-100 spectrometer was used without an entrance slit. The PMT signals were collected and digitized in a LeCroy 9361 300 MHz oscilloscope then transmitted to a PC. Lifetime data were analyzed with software written specifically for this system by OLIS, Inc. The decay times reported in Table 1 are either based on the best single exponential fits or they are amplitude-weighted averages based on the amplitude of the fitted components. The mean decay times were longer for higher energy than lower energy excitation and for the higher energy components for all the complexes. In the complexes for which the emission components could be somewhat resolved, the lowest energy component had a shorter lifetime but was much more sensitive to am(m)ine deuteration.[22]

D. MMCT Bandshape Interpretation. The emission band is interpreted as the sum of Gaussian functions representing a fundamental component, $I_{\nu_m(f)}$, and the vibronic components that are determined by the differences in ground and excited-state molecular geometries,[46−48]

$$I_{\nu_m} \cong I_{\nu_m(f)} + I_{\nu_m(0'1)} + I_{\nu_m(0'2)} + I_{\nu_m(0'3)} + \ldots \quad (4)$$

Procedures for deconvoluting $I_{\nu_m(f)}$ from the observed emission spectrum have been described in detail previously,[35,46,48] and they are based on a careful Grams32 fitting of a Gaussian function, $I_{\nu_m(em)}$, to the high energy side of the experimental emission spectrum divided by the emission energy ($I_{\nu_m(em)}$),[17,19,47,48] such that $I_{\nu_m(f)}$ closely matches the slope of the high energy side of $I_{\nu_m(em)}$ and accounts for more than 80% of the intensity of the high energy emission spectral component. Provided that the emission sideband amplitudes are relatively small and that the component bandwidths are less than about 1000 cm^{-1}, the energy maximum of $I_{\nu_m(f)}$, $h\nu_{max(f)}$, provides an experimental estimate of $E_{eg}^{0'0}$ and $I_{\nu_m(f)} \cong I_{\nu_m(0'0)}$. The amplitude of this component contains weighting parameters, as well as many physical constants, matrix element contributions, and so forth, that are common to all the emission components.[17,19,47,48,66]

$$I_{\nu_m(0'1)} \cong I_{\max(f)} \sum_i \left(\frac{\lambda_i}{h\nu_i}\right) e^{-[G_i/w]^2} \quad (5)$$

$$G_i = h\nu_{\max(f)} - h\nu_i - h\nu_m$$

$$I_{\nu_m(0'2)} \cong \frac{I_{\max(f)}}{2} \sum_i \sum_j \left(\frac{\lambda_i}{h\nu_i}\right)\left(\frac{\lambda_j}{h\nu_j}\right) e^{-[G_{ij}/w]^2} \quad (6)$$

$$G_{ij} = h\nu_{\max(f)} - h\nu_i - h\nu_j - h\nu_m$$

where $(\Delta\nu_{1/2})^2 = 4(\ln 2)w^2$ is the full width of $I_{\nu_m(f)}$ at half its maximum height,[47,48] This methodology has been substantiated by combining the respective $I_{\nu_m(f)}$ components obtained from the 77 K emission spectra of $[Ru(NH_3)_4bpy]^{2+}$[30] and $[Ru(bpy)_3]^{2+}$ with the individual vibronic components derived from resonance-Raman (rR) parameters reported for these complexes[30,32] to construct rR-based emission spectra whose bandshapes agree very well with those found experimentally.[48,50] The emission bandshapes are most conveniently discussed in terms of the normalized difference spectral amplitudes,

$$A_{\nu_m(diff)} = \frac{I_{\nu_m(m)} - I_{\nu_m(f)}}{I_{\max(f)}} \quad (7)$$

The 77 K emission spectra are typically weakly structured, broad envelopes, and these can be interpreted in terms of the sum over the corresponding vibronic contributions of the displacement modes, k, which are convoluted when $\Delta h\nu_k < \sim\Delta\nu_{1/2}$ as is the case for the metal−ligand vibrational modes of the complexes discussed here.

Results

A. General Information. The ambient MMCT absorption spectra are very intense, broad, and more symmetrical than the 77 K emission spectra for all of these complexes as is illustrated in Figure 3.[41,42] Thus, the Gaussian analysis of the ambient MMCT absorption bands of the *trans*-$[([14]aneN_4)Cr\{CNRu(NH_3)_5\}_2]^{5+}$ complex was surprisingly

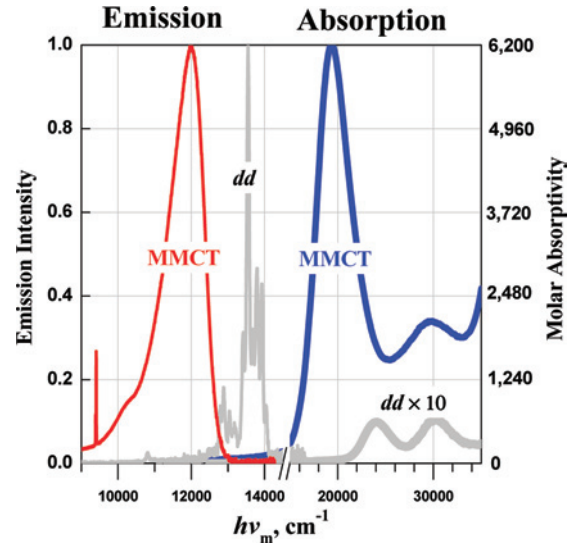

Figure 3. Comparison of the ambient absorption (in water; blue curve) and 77 K emission spectra (in DMSO/water; red curve) of $[([14]aneN_4)Cr\{(CNRu(NH_3)_5\}_2]^{5+}$ and $[([14]aneN_4)Cr(CN)_2]^+$ (gray curves). Except for the *dd* absorption spectrum, the maximum spectral intensities are normalized to 1.0 in this comparison. Note the difference in the energy scale for emission and absorption.

(66) Myers, A. B.; Mathies, R. A.; Tannor, D. J.; Heller, E. J. *J. Chem. Phys.* **1982**, *77*, 3857.

Table 2. Summary of Spectroscopic Observations on Cr(CN)Ru MMCT Excited States

complexes	MMCT absorption λ_{max}, nm (cm^{-1} /10^3) [$\varepsilon/10^3$][a]	MMCT emission, (0′−0) [$\Delta\nu_{1/2}$][b]	(^{2}E)Cr^{III} parent[c]	$^2Cr^{III}$ complex[d]	k_d, (μs)$^{-1}$[e]
$[Cr(NH_3)_5\{CNRu(NH_3)_5\}]^{4+}$	462(21.6)[3.5]	12.8 ± 0.2[f] (12.5 ± 0.2) [1.1][g]	14.72 [14.52][h]	13.6	0.83
$[Cr(ND_3)_5\{CNRu(ND_3)_5\}]^{4+}$		12.8 ± 0.2[i]	14.73		0.036
trans-$[Ru(NH_3)_4\{NCCr(NH)_5\}_2]^{6+}$	430(23.2)(6.2)	13.2, 13.3 [j](13.3 ± 0.1) [0.91][g]	14.72 [14.52][h]	13.8	
trans-$[Cr([14]aneN_4)\{CNRu(NH_3)_5\}_2]^{5+}$[k]	507(19.7)[8.0]	11.97 ± 0.05 (12.02) [0.72]	14.03		1.3
trans-$[Cr(d_4$-$[14]aneN_4)(CNRu(ND_3)_5)_2]^{5+}$[l]		11.98 ± 0.05 (12.06) [0.72]	14.04		0.094
trans-$[Cr(ms$-5,12-$Me_6[14]aneN_4)\{CNRu(NH_3)_5\}_2]^{5+}$	522(19.2)[8.2]	11.84 ± 0.05 (11.916) [0.763]	14.074	13.51	0.86
trans-$[Cr(d_4$-*ms*-5,12-$Me_6[14]aneN_4)\{CNRu(ND_3)_5\}_2]^{5+}$		11.82 ± 0.05 (11.91) [0.75]			0.051
cis-$[Cr(rac$-5,12-$Me_6[14]aneN_4)\{CNRu(NH_3)_5\}_2]^{5+}$	525(19.0)[8.0]	11.30 ± 0.05 (11.41) [0.76]	13.852	12.9	
cis-$[Cr(bpy)_2\{CNRu(NH_3)_5\}_2]^{5+}$	655(15.3)[6.0][m]	7.9 ± 0.1 (7.94) [0.8]	13.22		
cis-$[Cr(bpy)_2(CNRu(ND_3)_5)_2]^{5+}$		7.5 ± 0.1 (7.60 ± 0.15)			

[a] Ambient absorption in water; all energies in $cm^{-1}/10^3$. [b] 77 K in butyronitrile except as indicated. [c] In the same solvent as the ruthenated complex. [d] Estimated energy of the $^2Cr^{III}$ emission component of the Cr(CN)Ru complex at 77 K. [e] Based on the MMCT excited-state lifetime at 77K in DMSO/water(D_2O) glasses. [f] DMSO/H_2O glass. [g] Highest intensity component of Grams32 deconvolution. [h] Modeled (^{2}E)Cr^{III} emission maximum for 500 cm^{-1} component bandwidths. [i] DMSO/D_2O glass. [j] For 512 and 473 nm excitations, respectively. [k] Reference 23. [l] Reference 22. [m] Watzky, M. A., Ph.D. Dissertation, Wayne State University, 1994.

simple since most of it was very well described by a single Gaussian component with a full-width at half height ($\Delta\nu_{1/2}$) of about 3.4×10^3 cm^{-1}. This is about 4.5 times larger than the 77 K emission bandwidth of this complex (i.e., $\Delta\nu_{1/2} =$ 763 cm^{-1} for the fundamental component) and more than twice as large as expected for the temperature dependence of a spectrum with a single vibronic component.[53] This is consistent with a previous suggestion that the unusually simple shapes of these ambient MMCT absorptions arise from the convolution of several different, but near in energy, electronic absorption components.[42]

As noted in our earlier reports,[12,22,23] most of the tetragonal $[(L)Cr^{III}(CN^-)Ru^{II}(L')]$ complexes exhibit weak, low energy ($h\nu_{max(em)} \sim (10-13) \times 10^3$ cm^{-1}) luminescence in DMSO/H_2O or butyronitrile glassy solutions at 77 K when irradiated in the region of their Ru^{II}/Cr^{III} MMCT absorption bands, and the emission maxima are 5000−7000 cm^{-1} lower energy than the absorption maxima (e.g., see Figure 3 and Table 2). The MMCT emissions differ in band shape and energy from the well-known (^{2}E)Cr^{III} emission spectra of these complexes (we use the O_h notation for simplicity; the degeneracy of the E(O_h) electronic states is removed in these systems),[60,65,67] as shown in Figures 3−5. Irradiations at higher energies typically result in emissions that are broadened on the high energy side or, in some cases, the generation of an emission component that is more typical of the (^{2}E)Cr^{III} emission (see Figure S1 in the Supporting Information).[12,22,23,68]

The low energy MMCT emission bands did not have Gaussian shapes; they were all broadened on the low energy side of the emission maximum so that a description of their bandshapes requires two or more Gaussian components. However, the dominant emission sideband intensities are found to be within 700 cm^{-1} of $h\nu_{max(f)}$, consistent with the dominant vibronic contributions arising from distortions in metal−ligand skeletal vibrational modes, that is, the maxima for $I_{\nu_m(diff)}$ typically occurred for $h\nu_d \sim 400-600$ cm^{-1} ($h\nu_d = h\nu_{max(f)} - h\nu_m$).

To assess the general effect of metalation on the ^{2}E emission we have prepared and examined the emission

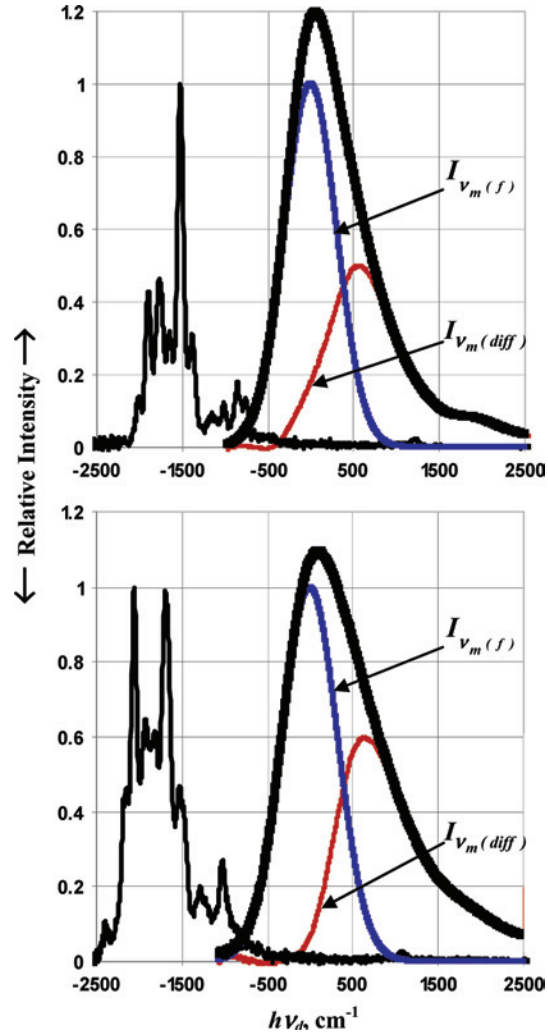

Figure 4. Comparison of the 77 K (DMSO/H_2O) emission and difference spectra of $[(MCL)Cr(CN)_2]^+$ (left) and $[(MCL)Cr\{(CNRu(NH_3)_5\}_2]^{5+}$ (right), where MCL = $[14]aneN_4$ (top panel) and *ms*-$Me_6[14]aneN_4$ (bottom panel). The dark blue Gaussians are the fundamental components inferred from the Grams32 fits, and the dark red curves are the differences, $I_{\nu_m(diff)}$, between these components and the emission spectra. The *dd* spectra are normalized so that their most intense vibronic components have $I_{max} = 1.0$, and the MMCT spectra are normalized so that $I_{max(f)} = 1.0$. Note that the abscissa is defined with respect to the maximum of the fundamental component, $h\nu_d = h\nu_{max(f)} - h\nu_m$.

behavior of the Hg^{2+} adduct of *trans*-$[Cr([15]aneN_4)(CN)_2]^+$.[22] The adduct emission was slightly shifted to higher

(67) Lessard, R. B.; Endicott, J. F.; Perkovic, M. W.; Ochrymowycz, L. A. *Inorg. Chem.* **1989**, *28*, 2574.
(68) Supporting information, see the paragraph at the end of this paper.

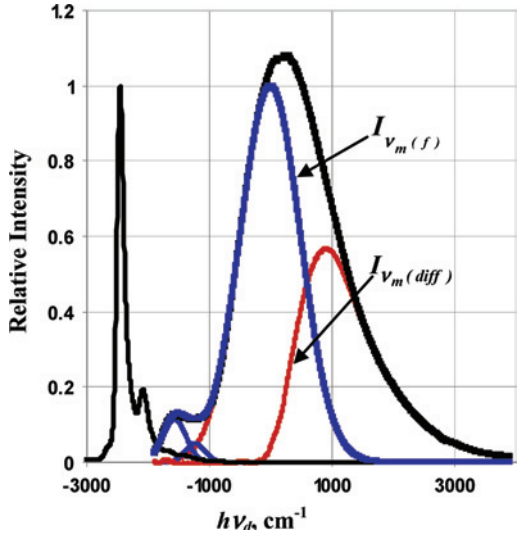

Figure 5. 77 K (DMSO/H_2O) emission and difference spectra of *cis*-$[(MCL)Cr(CN)_2]^{5+}$ (left) and *cis*-$[(MCL)Cr\{(CNRu(NH_3)_5\}_2]^{5+}$ (right), where MCL = *rac*-$Me_6[14]aneN_4$. The *dd* emission spectrum is normalized so that the $\{e,0'\}\rightarrow\{g,0\}$ component has $I_{max} = 1.0$, and the MMCT spectra are normalized so that $I_{max(f)} = 1.0$. For other details see the caption of Figure 4.

energy and very slightly broadened (Figure S2 in the Supporting Information).[68]

B. Emission Spectra of the Complexes. 1. *trans*-$[(MCL)Cr\{CNRu(NH_3)_5\}_2]^{5+}$ Complexes (MCL = $[14]aneN_4$ and ms-$Me_6[14]aneN_4$). The MMCT spectra of these complexes are compared to the *dd* emission spectra of their *trans*-$[Cr(MCL)(CN)_2]^+$ parent complexes in Figure 4. The high energy rise of the 77 K emission spectra of these complexes is very easily fitted to a fundamental Gaussian component as is shown in the figure. Note that the $\{e(^2E),0'\}\rightarrow\{g,0\}$ component is forbidden in the emission of the centrosymmetric complexes.

2. *cis*-$[(rac\text{-}Me_6[14]aneN_4)Cr\{CNRu(NH_3)_5\}_2]^{5+}$ Complex. The 77 K (DMSO/H_2O; 1:1, v/v) emission and difference spectra of this complex are shown in Figure 5. The emission bandwidth is large relative to that of the other $[(MCL)Cr\{(CNRu(NH_3)_5\}_2]^{5+}$ complexes (Table 2 and Figures 5 and 6), and fitting of a fundamental component was slightly more difficult owing to this and to the weak feature at the high energy foot of the emission spectrum. We attribute the latter feature to emission from a Cr^{III}-centered component of the lowest energy adiabatic excited state of the complex, $^2Cr^{III}$, that is red-shifted as a result of configurational mixing with an MMCT excited state. This high energy feature is analogous to but weaker relative to the MMCT component of the emission than found for the high energy $(^2E)Cr^{III}$ spectral contribution that results when the *trans*-$[(ms\text{-}Me_6[14]aneN_4)Cr\{CNRu(NH_3)_5\}_2]^{5+}$ complex is irradiated at energies that are higher than the MMCT absorption band (Figure S1 in the Supporting Information).[22] Although their bandwidths and some minor details vary, the MMCT emission spectral bandshapes of the $[(MCL)Cr\{CNRu(NH_3)_5\}_2]^{5+}$ complexes are very similar, as shown in Figure 6, while the $(^2E)Cr^{III}$emission spectra of their parent complexes are very different because the $\{e(^2E),0'\}\rightarrow\{g,0\}$ component is

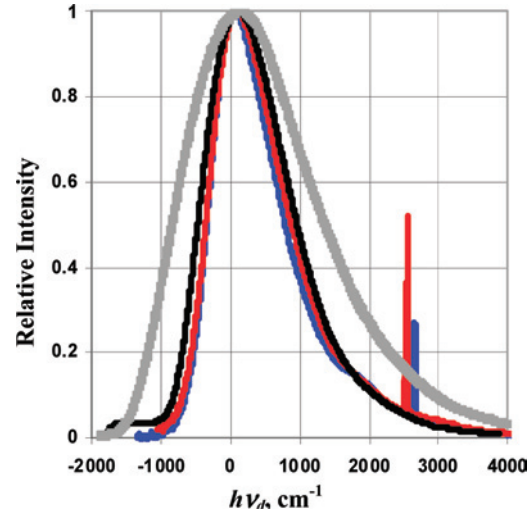

Figure 6. Comparison of the 77 K (DMSO/H_2O) MMCT emission spectra of the *trans*- and *cis*-$[(MCL)Cr\{(CNRu(NH_3)_5\}_2]^{5+}$ and the $[(NH_3)_5Cr\text{-}\{CNRu(NH_3)_5\}]^{4+}$ (gray curve) complexes, where MCL = $[14]aneN_4$ (blue curve), *ms*-$Me_6[14]aneN_4$ (red curve) and *rac*-$Me_6[14]aneN_4$ (black curve). The MMCT spectra are normalized so that $I_{max(em)} = 1.0$. Note that the abscissa is approximately defined with respect to the maximum of the MMCT fundamental emission component but adjusted so that the emission maxima approximately coincide.

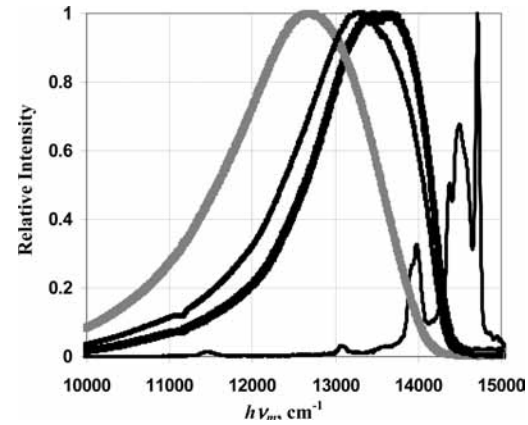

Figure 7. Comparison of the 77 K (DMSO/H_2O) emission spectra of (from left to right): $[(NH_3)_5Ru\{(NC)Cr(NH_3)_5\}]^{4+}$, $[(NH_3)_4Ru\{(NC)Cr(NH_3)_5\}_2]^{6+}$ with 532 nm excitation, $[(NH_3)_4Ru\{(NC)Cr(NH_3)_5\}_2]^{6+}$ with 473 nm excitation, and $[Cr(NH_3)_5(CN)]^{2+}$.

allowed (and most intense) in the non-centrosymmetric *cis*-$[(rac\text{-}Me_6[14]aneN_4)Cr\{CNRu(NH_3)_5\}_2]^{5+}$ complex.

3. $[(NH_3)_5Cr\{CNRu(NH_3)_5\}]^{4+}$ and *trans*-$[(NH_3)_4Ru\text{-}\{NCCr(NH_3)_5\}_2]^{6+}$ Complexes. The 77 K emission spectra of these complexes were significantly broader than those of the other complexes reported here, but the slopes of the high energy side of the emission bands were steeper than expected for the overall band breadth. It was not possible to fit the spectra using our usual procedure with a dominant high energy Gaussian component whose bandwidth was adjusted to match to the high energy spectral curvature (see Figure 7). The best fits of these spectra were obtained for relatively weak and narrow high energy components such as shown in Figure S3 (Supporting Information).[68] Because the emission bands were so broad, their fundamental components could not be identified with certainty. The fits shown in

Figure S4 of the Supporting Information[69] were obtained by restricting them to four or five Gaussian components and allowing one or two high energy components to have relatively narrow bandwidths. With these restrictions, reasonably similar parameters were obtained for the emission spectra as shown in Figure S3 and Table S4 in the Supporting Information.[68] The emission spectrum of the *trans*-$[(NH_3)_4Ru\{NCCr(NH_3)_5\}_2]^{6+}$ complex has two dominant overlapping components whose relative intensities changed with the excitation energy. In view of the overlap of the parent $[Cr(NH_3)_5CN]^{2+}$ *dd* and the complex MMCT emission spectra, and since the excited-state lifetimes of $[(NH_3)_5Cr\{CNRu(NH_3)_5\}]^{4+}$ are excitation energy dependent,[12] the higher energy emission components are most likely analogous to the high energy emission components found for the $[(MCL)Cr\{CNRu(NH_3)_5\}_2]^{5+}$ complexes, discussed above and previously,[12,22,23] and thus have predominately the characteristics of a Cr^{III}-centered emission ($^2Cr^{III}$). If there is significant MMCT/*dd* configurational mixing in the CrCNRu complexes, then any *dd* component of the spectrum is expected to be broadened. To simulate the effect of such broadening, we have assigned each of the more significant *dd* emission components of the $[Cr(NH_3)_5CN]^{2+}$ emission spectrum a bandwidth of 500 cm^{-1}; this results in an emission envelope that is not Gaussian with $h\nu_{max(dd)} \approx 14{,}540$ cm^{-1} and a bandwidth of ~ 756 cm^{-1}.

If we assume *dd*/MMCT configurational mixing and a double minimum in the lowest energy adiabatic electronic excited state with emission possible from each of those minima, then the highest energy deconvoluted components would have largely metal-centered character and lower energy than the parent complex emission origin by about 1100 and 500 cm^{-1}, respectively, for $[(NH_3)_5Cr\{CNRu(NH_3)_5\}]^{4+}$ and *trans*-$[(NH_3)_4Ru\{NCCr(NH_3)_5\}_2]^{6+}$ as indicated in Table S4 (Supporting Information;[68] this involves using two Gaussian *dd* components to approximately fit the non-Gaussian envelope of Cr(III) *dd* emission components). This assignment leads to similar fundamental MMCT components with $\Delta\nu_{1/2} = 912$ cm^{-1} and $h\nu_{max(f)} = 12{,}500 \pm 100$ and $13{,}300 \pm 100$ cm^{-1}, respectively, for the bimetallic and trimetallic complexes (see Table 1 and the Supporting Information, S4).[68]

4. $[(bpy)_2Cr\{CNRu(NH_3)_5\}_2]^{5+}$ Complex. The emission of this complex is the weakest, by orders of magnitude, of all the complexes reported here. There is an apparent emission in the 7500−8000 cm^{-1} spectral region (a region in which the OMA V is very sensitive), but the signal-to-noise ratio is poor and complex emission is difficult to separate from scattered excitation laser light. The details of our observations are summarized briefly below (see also the Supporting Information, S5).[68]

The MMCT absorption band of this complex has its maximum at 655 nm ($\varepsilon_{max} = 8{,}000$ M^{-1} cm^{-1})[42] and irradiations of the complex at appreciably higher energy than the MMCT absorption (532 nm) did not result in signals that could be reliably distinguished from the noise. Better signals were obtained with 658 nm irradiations (Newport LPM658-65E, 65 mW diode laser module); however, the observations with this source are complicated by the relatively intense second order dispersion of scattered light which was a larger problem than usual because of the very weak sample emission and because this weak emission forced us to use the stronger NIR emissions of $[Ru(acac)_2bpy]$ to "optimize" the optical bench alignment for each experiment. Consequently, we have obtained "background" spectra, with only solvent in the sample cell for each experiment, and these background spectra were subtracted from the sample signals. Since these spectra were obtained with samples in 2 mm cylindrical fluorescence cells which were placed in a liquid nitrogen bath of the spectroscopic Dewar flask, the details of the scattered light were not rigorously reproducible and some additional corrections were often necessary (using Grams32). We have assumed that there is no scattered light correction at 10,000 cm^{-1} (see the Supporting Information, S5).[68] When the scattered light components are removed, a reasonably typical MMCT emission profile results as shown in Figure 8: $h\nu_{max(em)} \approx 7{,}860$ cm^{-1}; $h\nu_{max(f)} \approx 7940$ cm^{-1}; $\Delta\nu_{1/2} \approx 800$ cm^{-1}.

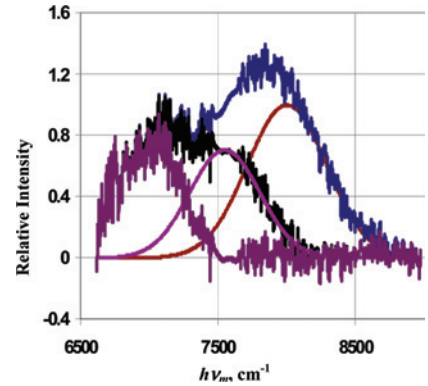

Figure 8. Resolved $[(bpy)_2Cr\{CNRu(NH_3)_5\}_2]^{5+}$ emission spectrum (dark blue). For the fundamental component (largest dark red Gaussian) $h\nu_{max(f)} = 8003$ cm^{-1}; $\Delta\nu_{1/2} = 681$ cm^{-1}. The difference spectrum is shown by the black curve (residual scattered light components at ~7600 cm^{-1} have been removed in Excel) and a Gaussian fit of the high energy side (dark red) is presumed to represent the envelope of 1st order metal−ligand vibronic terms; $h\nu_{max(lf)} = 7550$ cm^{-1}; $\Delta\nu_{1/2} = 601$ cm^{-1}. The remainder spectrum (purple) produced by subtracting the two Gaussians from the emission is a measure of the quality of the Gaussian fits.

Our other attempts resulted in emission spectra for this complex that were qualitatively in agreement with that shown in Figure 8, but their signal-to-noise ratios were worse (Supporting Information, S5).[68] The average of the most intense signals resulted in resolved spectra with $h\nu_{max(em)} \approx 7500 \pm 100$ cm^{-1}, $h\nu_{max(f)} \approx 7{,}600 \pm 150$ cm^{-1}, and $\Delta\nu_{1/2} \approx 600$ cm^{-1}. Ammine perdeuteration did not significantly improve the signal quality but it did shift the emission maximum to lower energy.

Discussion

This is the first detailed examination of the electron transfer emission spectra generated from the irradiations of a simple class of transition metal-donor/transition metal-acceptor complexes. These emissions are typically in the near-infrared

(69) This envelope is constructed as a best fit to the part of the $[Ru(NH_3)4bpy]^{2+}$ difference spectrum that cannot be attributed to vibronic contributions from bpy ligand distortions.[50]

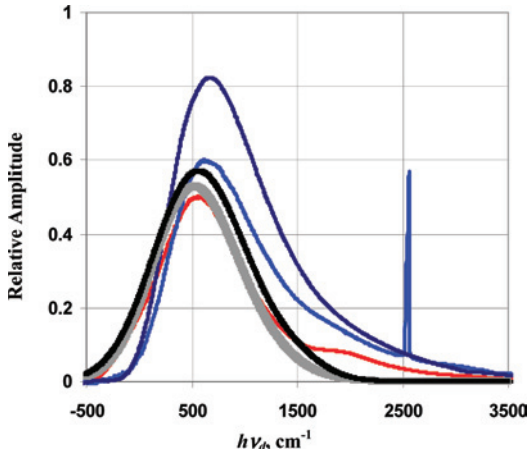

Figure 9. Comparison of difference spectra of the *trans*-[(MCL)Cr(CNRu(NH$_3$)$_5$}$_2$]$^{5+}$ (MCL = [14]aneN$_4$, red; *ms*-Me$_6$[14]aneN$_4$, blue) and *cis*-[(*rac*-Me$_6$[14]aneN$_4$)Cr(CNRu(NH$_3$)$_5$}$_2$]$^{5+}$ (dark blue) with the envelope of metal−ligand stretching contributions inferred from the [Ru(NH$_3$)$_4$bpy]$^{2+}$ (black) and [Ru([14]aneN$_4$)bpy]$^{2+}$ (gray) emission spectra. The very narrow peak in some spectra at $\nu_d \sim 2500$ cm^{-1} is the result of 2nd order scattered radiation from the diode laser used for excitation.

spectral region with very large H/D isotope effects and in this series of complexes they are complicated by configurational mixing with the near in energy Cr^{III}-centered excited state(s). In view of their uniqueness, several features of the emission spectra are considered in detail.

A. Characterization of the 77 K Emission Spectra. 1. MMCT Bandshapes of the [(MCL)Cr{CNRu(NH$_3$)$_5$}$_2$]$^{5+}$ Complexes. The MMCT emission sideband-shapes of these complexes are all very similar as is shown in Figure 9, although their differences in $\Delta\nu_{1/2}$ do result in some amplitude variations (a consequence of the increased overlap of spectral components with increasing bandwidth when $\Delta h\nu_k < \Delta\nu_{1/2}$).[48] Furthermore, the overall shapes of these sidebands, as well as the energies and amplitudes of their maxima ($h\nu_{max(lf)}$ and $A_{max(lf)}$, respectively), are surprisingly similar to the envelope of metal−ligand vibronic contributions inferred from the emission of the [Ru(NH$_3$)$_4$bpy]$^{2+}$ complex[50,69] as shown in Figure 9. Thus, the energies of these maxima are consistent with distortions in the metal−ligand vibrational modes of the complexes, and the small amplitudes and similar shapes of the [(MCL)Cr{CNRu(NH$_3$)$_5$}$_2$]$^{5+}$ and [Ru(NH$_3$)$_4$bpy]$^{2+}$ complexes indicate that the metal−ligand distortions in the MMCT excited state are small in amplitude. This can only be the case if the Cr^{II} centers of these complexes have a low spin electronic configuration (t_{2g}^4 in O_h symmetry; $b_2^2e^2$ or b_2e^3 in C_{4v} symmetry).

2. Bandshapes of the Remaining Complexes. The emission bandshapes of the [(NH$_3$)$_5$Ru{(NC)Cr(NH$_3$)$_5$}]$^{4+}$ and [(NH$_3$)$_4$Ru{(NC)Cr(NH$_3$)$_5$}$_2$]$^{6+}$ complexes are relatively broad on the high energy side of their emission bands and the high energy contribution is more intense for higher excitation energies as is typical for this family of Cr(CN)Ru complexes, but we have not been able to resolve their "pure" MMCT components. We attribute this problem to the relatively small energy differences between the MMCT and the (^{2}E)Cr^{III} emission components (see Table 2), and we have estimated the various components based on this interpretation and a Grams32 deconvolution of the spectra.

The [(bpy)$_2$Cr{CNRu(NH$_3$)$_5$}$_2$]$^{5+}$ emission is extremely weak, but the emission band shape appears to be similar to those of the [(MCL)Cr{CNRu(NH$_3$)$_5$}$_2$]$^{5+}$ complexes discussed above.

3. Characterization of the (^{2}E)Cr^{III} Contributions. The estimated electronic origins of the MMCT emission bands ($h\nu_{max(f)}$) of most of these complexes are within 2500 cm^{-1} of the (^{2}E)Cr^{III} emission band origin of the corresponding parent complex; the exception is [(bpy)$_2$Cr{CNRu(NH$_3$)$_5$}$_2$]$^{5+}$ for which this energy difference appears to be more than about 5000 cm^{-1}. If there is only a small amount of configurational mixing between the lowest energy MMCT and (^{2}E)Cr^{III} excited states of the complex, then the lowest energy electronic excited state can be represented by an adiabatic PE surface with two local minima, and the properties of the complex at the respective minima will correspond to the slightly modified properties of the respective diabatic (or unmixed) excited states, as qualitatively illustrated in Figure 1. Such an excited state is analogous to a ground-state "mixed valence" complex, and we have previously reported on the emission bandshapes of similar, but more symmetrical "mixed valence" MLCT excited states, [Ru^{III}{(PP$^-$)Ru^{II}}] (PP a polypyridyl ligand such as dpp = 2,3-(2-pyridyl)pyrazine), of PP-bridged bimetallic-Ru^{II} complexes.[70,71] The Ru^{II}{(NC)Cr^{III}} complexes contrast to the Ru-(PP) complexes because the diabatic (^{2}E)Cr^{III} excited-state moiety has the ground-state nuclear coordinates while the Cr^{II}, Ru^{III}, and (PP$^-$) moieties in the respective CT excited states do not. One result of this feature of the (^{2}E)Cr^{III} excited state is that (^{2}E)Cr^{III}/MMCT configurational mixing will reduce the distortion in the adiabatic MMCT excited state.

Irradiations at energies less than the MMCT absorption band maxima of this class of complexes usually lead to a well resolved MMCT emission as illustrated in Figures 3−7, while irradiations at energies that are significantly higher than the MMCT absorbance typically result in a slightly longer lived emission with appreciable spectral contributions on the high energy side of the MMCT emission.[12,22,23] These high energy components typically have somewhat smaller isotope effects than do the MMCT components, and both the lifetimes and isotope effects are intermediate between the corresponding properties of the resolved MMCT components and the (^{2}E)Cr^{III} parent complex emissions.[12,22,23] The partial resolution of the high energy ((^{2}E)Cr^{III}-like) emission component of the *trans*-[(*ms*-Me$_6$[14]aneN$_4$)Cr{CNRu(NH$_3$)$_5$}]$^{5+}$ complex has been discussed previously, and the approximately 500 cm^{-1} shift to lower energy of this emission component relative to the parent *trans*-[(*ms*-Me$_6$[14]aneN$_4$)Cr(CN)$_2$]$^+$ emission[22] is in very good qualitative agreement with significant excited state/excited state configurational mixing and the argument that the lowest energy adiabatic excited-state PE surfaces of most of these complexes have double minima such as represented in Figure 1. A similar, but relatively weaker ^{2}Cr^{III} emission component may occur in the *cis*-[(*rac*-Me$_6$[14]aneN$_4$)Cr{CNRu-

(70) Chen, Y.-J.; Endicott, J. F.; Swayambunathan, V. *Chem. Phys.* **2006**, *326*, 79.
(71) Endicott, J. F.; Chen, Y.-J. *Inorg. Chim. Acta* **2007**, *360*, 913.

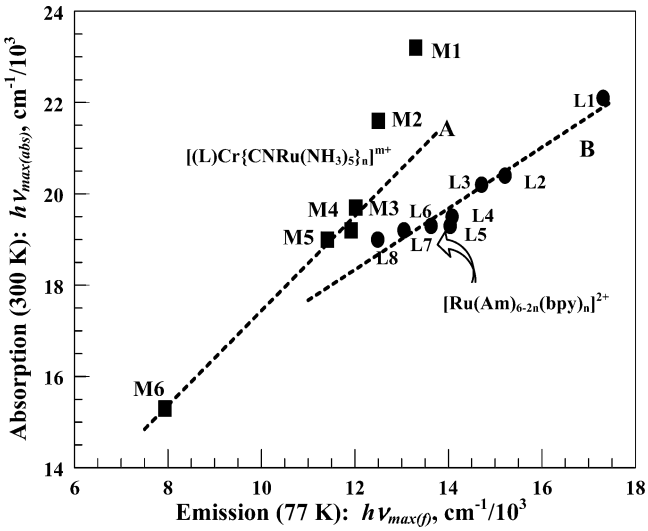

Figure 10. Correlation of the ambient $[(L)Cr\{CNRu(NH_3)_5\}_n]^{(3+n)+}$ MMCT (squares) and $[Ru(Am)_{6-2n}(bpy)_n]^{2+}$ MLCT (circles) absorptions with the respective 77 K fundamental emission components. For the $[(L)Cr\{CNRu(NH_3)_5\}_n]^{(3+n)+}$ complexes: *trans*-$[(NH_3)_4Ru\{NCCr(NH_3)_5\}_2]^{5+}$, M1; $[(NH_3)_5Cr\{CNRu(NH_3)_5\}]^{4+}$, M2; *trans*-$[([14]aneN_4)Ru\{NCCr(NH_3)_5\}_2]^{5+}$, M3; *trans*-$[(ms\text{-}Me_6[14]aneN_4)Ru\{NCCr(NH_3)_5\}_2]^{5+}$, M4; *cis*-$[(rac\text{-}Me_6[14]aneN_4)Ru\{NCCr(NH_3)_5\}_2]^{5+}$, M5; *cis*-$[(bpy)_2Ru\{NCCr(NH_3)_5\}_2]^{5+}$, M6. For $[Ru(Am)_{6-2n}(bpy)_n]^{2+}$ [(Am); *n*]:[46] [3], L1; [(en); 2], L2; $[(NH_3)_2$; 2], L3; [(*rac*-$Me_6[14]aneN_4$); 1], L4; [($[14]aneN_4$); 1], L5; [($[15]aneN_4$); 1], L6; $[(en)_2$; 1], L7; $[(NH_3)_4$; 1], L8. The least-squares lines (in cm^{-1}) are (A, excluding M1 and M2) $(1.03 \pm 0.06)h\nu_{max(f)} + (6.5 \pm 0.8)$; and (B) $(0.67 \pm 0.07)h\nu_{max(f)} + (10.3 \pm 0.4)$.

$(NH_3)_5\}]^{5+}$ emission spectrum, but this feature has not been as well characterized. We estimate that the differences in the MMCT and parent $(^2E)Cr^{III}$ emission band origins are smallest for $[(NH_3)_5Cr\{CNRu(NH_3)_5\}]^{4+}$ and *trans*-$[(NH_3)_4Ru\{NCCr(NH_3)_5\}_2]^{5+}$ complexes, and there appears to be correspondingly more overlap of the $(^2E)Cr^{III}$-like and MMCT-like components in the emission spectra of these complexes.

4. MMCT Excited-State Energies. The energy maxima of the resolved MMCT fundamental components, $h\nu_{max(f)}$, which are estimates of the electronic origins, correlate well with the MMCT absorption maxima as shown in Figure 10.

The correlation of the energies of the $[(L)Cr\{CNRu(NH_3)_5\}_n]^{(3+n)+}$ absorption maxima with $h\nu_{max(f)}$ in Figure 10 is significantly steeper than that for the $[Ru(Am)_{6-2n}(bpy)_n]^{2+}$ complexes. Since the relatively shallow slope of the latter has been attributed to a systematic increase in the inter-atomic exchange energy as bpy ligands are replaced by am(m)ines,[19,46−48,72] the comparison in Figure 10 suggests that (a) there is little difference in the net exchange energies, K_{exch}, of the relevant quartet and doublet $[(L)Cr^{II}\{CNRu^{III}(NH_3)_5\}_n]^{(3+n)+}$ excited states of the complexes; and/or (b) that there is relatively little variation in K_{exch} through the series of complexes. Another important feature of these systems that is illustrated by Figure 10 is that the pseudo-Stokes shift, $E_{PSS} = h\nu_{max(abs)} - h\nu_{max(f)}$ ($\sim \Delta E_{eg}$ in eq 2), is 1000−3000 cm^{-1} larger for the $[(L)Cr\{CNRu(NH_3)_5\}_n]^{(3+n)+}$ than for the $[Ru(Am)_{6-2n}(bpy)_n]^{2+}$ complexes. In the simplest limit that the Franck−Condon excited state populated by absorption and the emitting state differ only in spin multiplicity and assuming that displacements in most solvent vibrational modes are frozen at 77 K, one expects that

$$E_{PSS} \approx \lambda_s + 2K_{exch} \quad (8)$$

The Franck−Condon excited state for the MLCT transitions has singlet and the emitting state triplet spin multiplicity so that $K_{exch} > 0$ (with typical values of several thousand wavenumbers)[72] for the $[Ru(Am)_{6-2n}(bpy)_n]^{2+}$ complexes. In contrast, the Franck−Condon and emitting excited states for the MMCT transitions have quartet and very likely doublet spin multiplicities, respectively, so that $K_{exch} < 0$. On this basis one would expect a smaller value of E_{PSS} for the emissions of the $[(L)Cr\{CNRu(NH_3)_5\}_n]^{(3+n)+}$ complexes than those of the Ru-bpy complexes, contrary to observation. One interpretation of this comparison is that ΔK_{exch} is very small for the relevant quartet and doublet $[(L)Cr^{II}\text{-}\{CNRu^{III}(NH_3)_5\}_n]^{(3+n)+}$ electronic excited states.

We have constructed the most shallow plausible correlation line for the $[(L)Cr\{CNRu(NH_3)_5\}_n]^{(3+n)+}$ complexes in Figure 10, and it is possible that the deviations from this correlation of the observations for the $[(NH_3)_5Cr\{CNRu(NH_3)_5\}]^{4+}$ and *trans*-$[(NH_3)_4Ru\{NCCr(NH_3)_5\}_2]^{5+}$ could be the result of more configurational mixing of their relatively high energy diabatic ^{2}MMCT excited states with a metal centered $(^2E)Cr^{III}$ excited state than is found for other complexes of this series. Alternatively, the most intense component of the emission may not correspond to the fundamental component for these complexes (such as would be expected if the emitting excited state contained a $^5Cr^{II}$ center), but this interpretation does not significantly improve the correlation for latter (trimetallic) complex.

The energies of CT excited states of coordination complexes almost always correlate strongly with the oxidation−reduction properties of their ground states.[18,73] Unfortunately, the lability of Cr^{II} complexes makes reductions of most Cr^{III} complexes electrochemically irreversible. The notable exceptions are the polypyridyl complexes of Cr^{III}. Thus, the reductions of all of the complexes reported here are electrochemically irreversible except for $[(bpy)Cr\{CNRu(NH_3)_5\}_2]^{5+}$. On the basis of the data in Table 1, we find that $F\Delta E_{1/2} = 0.99$ eV (8,000 cm^{-1}) which is very similar to the emission energy in Table 2. However, the 77 K emission energies for the $[Ru(Am)_{6-2n}(bpy)_n]^{2+}$ complexes are smaller than their corresponding values of $F\Delta E_{1/2}$, as illustrated in Figure 11, largely as a result of the inter-atomic exchange energy contributions.[19,48,70] Thus, the observations in Figures 10 and 11 can be most simply reconciled if (a) the MMCT absorption generates a Franck−Condon excited state of quartet spin multiplicity in which K_{exch} is much smaller than the intra-atomic exchange energy of the ground state (~15,000 cm^{-1} for $^4Cr^{III}$); and (b) if the[4,2] $[(L)Cr^{II}\{CNRu^{III}(NH_3)_5\}_n]^{(3+n)+}$ excited states that are relevant to these correlations have the same orbital populations and differ only in the orientations of the spin moments at

(72) Lever, A. B. P.; Gorelsky, S. I. *Coord. Chem. Rev.* **2000**, *208*, 153.

(73) Lever, A. B. P.; Dodsworth, E. In *Electronic Structure and Spectroscopy of Inorganic Compounds*; Lever, A. B. P., Solomon, E. I., Eds.; Wiley: New York, 1999; Vol. II, pp 227.

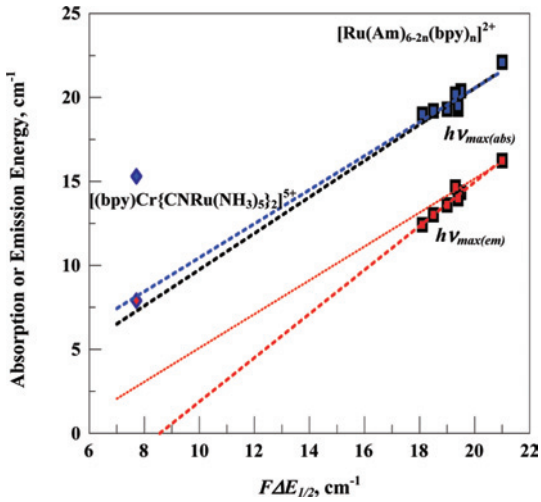

Figure 11. Correlation of absorption (blue) and emission (red) maxima for $[Ru(Am)_{6-2n}(bpy)_n]^{2+}$ (squares) and $[(bpy)Cr\{CNRu(NH_3)_5\}_2]^{5+}$ (diamonds) complexes. The points for the $[Ru(Am)_{6-2n}(bpy)_n]^{2+}$ complexes are sequenced as in Figure 10.

their Cr^{II} and Ru^{III} centers. This possibility is developed further below.

5. Effects of N−H/N−D Isotopic Substitution. In principle, am(m)ine perdeuteration can alter both the emission energy and excited-state lifetime. The emission energy is altered through the zero point energy (*zpe*) when some vibrational modes differ in frequency in the ground and excited states. In general, the N−H vibrational frequencies are larger when the am(m)ine ligand is coordinated to a +2 metal ion than when it is coordinated to a +3 metal ion;[74] however, when both metals involved in a MMCT transition have am(m)ine ligands, these differences tend to cancel and the observed effects of deuteration on emission energies are quite small. Nevertheless, there is a systematic trend for the difference in the differences of *zpe*'s, ∇zpe, for the emission maxima to decrease as the difference between the numbers of N−H moieties coordinated to Cr and Ru increases; thus, for the complexes in Table 2 ($\Delta N = N$(Ru−N−H) − N(Cr−N−H), considering only one Ru center in each complex) $[(NH_3)_5Cr\{CNRu(NH_3)_5\}]^{4+}$, $\Delta N = 0$, $\nabla zpe = -70 \pm 20$ cm^{-1}; $[(MCL)Cr\{CNRu(NH_3)_5\}_2]^{5+}$, $\Delta N = 11$, $\nabla zpe = 15 \pm 20$ cm^{-1}; $[(bpy)_2Cr\{CNRu(ND_3)_5\}_2]^{5+}$, $\Delta N = 15$, $\nabla zpe = 400 \pm 200$ cm^{-1}. These observations indicate that there is a larger difference in the N−H force constants for the Cr^{III}-*Cr^{II} couple than for the Ru^{II}-*Ru^{III} couple (asterisk indicates the excited-state moiety). The very large ∇zpe for the last of these complexes is remarkably close to expectation since ν_g(NH) ≅ 3077 and 3320 cm^{-1}, respectively, for the ground states of $[Ru(NH_3)_6]^{3+}$ and $[Ru(NH_3)_6]^{2+}$,[74] in the absence of any significant configurational mixing and assuming similar N−H vibrational frequency differences for the $Ru(NH_3)_6$ moieties of the $CrCNRu(NH_3)_5$ complexes, the shift in *zpe* upon ammine deuteration of a single vibrational mode (k) is

$$(\nabla zpe)_k \approx \frac{1}{2}h[\nu_{g(d)} - \nu_{e(d)}]_k\delta + ... \qquad (9)$$

where $\delta = (1 - 2^{-1/2})$. For 15 N−H vibrational modes all with the same difference in ground and excited-state vibrational frequencies (≈ 240 cm^{-1}), eq 9 predicts $\nabla zpe \approx$ 444 cm^{-1}.

With the exception of $[(bpy)_2Cr\{CNRu(ND_3)_5\}_2]^{5+}$, the excited-state lifetimes of these complexes increase 10−30 fold upon am(m)ine perdeuteration.[12,22,23] However, the displacements in the N−H nuclear coordinates are very small (the maximum amplitudes of the envelopes of N−H vibronic components are ≤30 cm^{-1}) which implies that the relaxation process involves some combination(s) of low frequency and high frequency displacement modes[22,23] (see section C below).

B. Implications for the MMCT Excited State(s). 1. Possible Electronic Configurations for Low Energy Excited States of $[(L)Cr\{CNRu(NH_3)_5\}_n]^{(3+n)+}$ Complexes. A $d\pi(Ru^{II}) \rightarrow d\pi(Cr^{III})$ electron transfer will initially generate an electronic triplet state of Cr^{II}. Since the emission spectra implicate such a "low spin" Cr^{II} species and because there are a very large number of possible Cr^{II}/Ru^{III} excited-state electronic configurations in these complexes, we will emphasize those electronic configurations which contain a local triplet state electronic configuration of Cr^{II} ($^3Cr^{II}$). There are 14 different MMCT excited states with a local $^3Cr^{II}$ configuration in C_{4v} symmetry (see Table S6 in the Supporting Information),[68] and those that will dominate the lowest energy, dipole allowed MMCT absorptions correspond to Franck−Condon excited states with $^4E[Cr^{II}(b_2e^3),Ru^{III}(b_2)]$, $^4B_2[Cr^{II}(b_2e^3),Ru^{III}(e^3)]$, and $^4E'[Cr^{II}(e^2),Ru^{III}(e^3)]$ electronic configurations; weaker contributions from the nominally symmetry forbidden transitions are also likely.

The excited states with the $^2X[Cr^{II}(b_2e^3),Ru^{III}(e^3)]$ electronic configurations (X = A_1, A_2, B_1, or B_2) are the most likely to be stabilized by bridging-ligand mediated superexchange coupling and configurational mixing with a $^2Cr^{III}$-centered excited state. Of these, the $^2A_1$(MMCT) and $^2B_1$(MMCT) states have the proper symmetry to mix with the lowest energy Cr^{III}-centered excited states, $^2A_1(Cr^{III})$ and $^2B_1(Cr^{III})$. Thus, this idealized symmetry-based argument suggests that LF/MMCT configurational mixing may play an important role in determining which electronic state has the lowest energy and that the electronic states that dominate the absorption may have different electronic orbital configurations from those of the states that dominate the emission. Furthermore, the lowest energy diabatic Cr^{III}-centered and MMCT excited states need not have the same symmetry so that in contrast to most simple mixed valence systems the PE minima of the lowest energy $^2Cr^{III}$ and ^{2}MMCT excited states may both be significantly stabilized by configurational mixing while their corresponding diabatic excited states may mix only very weakly with one another. The simple energy level scheme in Figure 12 illustrates these features.

Figure 12 illustrates the importance of both exchange energies and configurational mixing in determining the lowest energy excited states. Thus, while most of the $^4Cr^{III}/^2Cr^{III}$ energy difference can be attributed to the large intra-atomic exchange energy contribution to the stability of the quartet ground state, the intra-atomic exchange energy contribution will be reduced and the inter-atomic contribution should be small since the net electronic spin is distributed over two

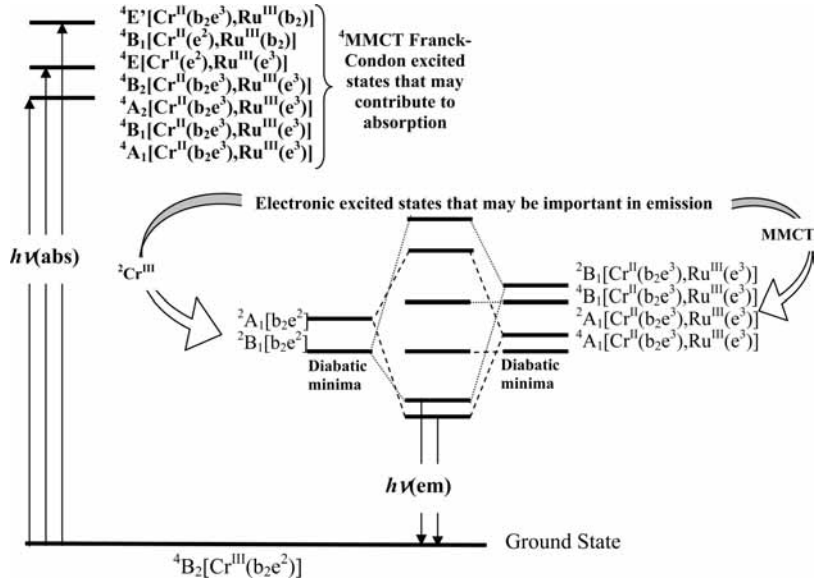

Figure 12. Qualitative scheme of electronic excited states in a bimetallic Cr(CNRu) complex with C_{4v} symmetry that may be important in absorption and emission. The states represented are those discussed in the text, and their relative energies and the energy differences are arbitrary. It is assumed that the diabatic MMCT excited states with $[Cr^{II}(b_2e^3),Ru^{III}(e^3)]$ electronic configurations do not differ greatly in energy but that those states with A_1 symmetry are slightly stabilized by means of weak π-bonding interactions. It is also assumed that the inter-atomic electron exchange energy between the partly occupied orbitals of Ru^{III} and Cr^{II} is very small owing to their spatial separation.

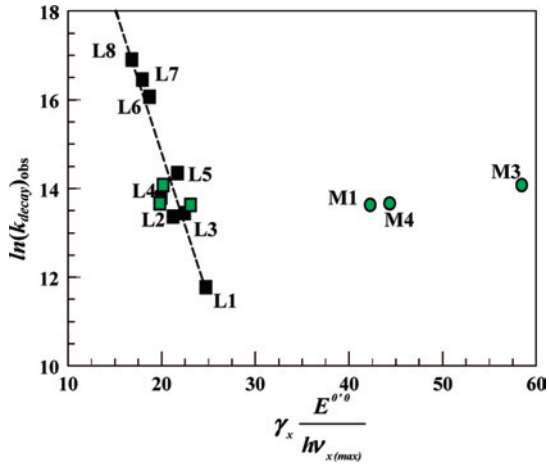

Figure 13. Comparison of the excited-state decay rate constants for $[Ru(Am)_{6-2n}(bpy)_n]^{2+}$ (black squares) and $[(L)Cr\{CNRu(NH_3)_5\}_n]^{(3+n)+}$ complexes. For this comparison $h\nu_x = 1440$ cm^{-1} and λ_x as in Table 2 for the Ru-bpy complexes; $h\nu_x \approx 450$ and $\lambda_x \approx 200$ cm^{-1} (Table 2), green circles, or $h\nu_x \approx 3000$ and $\lambda_x \approx 30$ cm^{-1}, green squares, for the Cr(CN)Ru complexes. For the least-squares line through the Ru-bpy data, $\ln(k_{decay})_{obsd} = (27 \pm 2) - (0.65 \pm 0.09)(\gamma_x E^{0'0}/h\nu_{x(max)})$. See the caption of Figure 10 for key to the complexes.

atoms that are separated by about 5.2 Å. Thus, the contributions of K_{exch} to the doublet and quartet $[Cr^{II}(b_2e^3),Ru^{III}(e^3)]$ excited-state electronic configurations may be similar, and the $^4A_1[Cr^{II}(b_2e^3),Ru^{III}(e^3)]$ and $^2A_1[Cr^{II}(b_2e^3),Ru^{III}(e^3)]^{5+}$ MMCT excited states are likely to have similar energies. However, configurational mixing with the lowest energy, diabatic $(^2E)Cr^{III}$ excited state would tend to result in greater stabilization of the ^{2}MMCT state. This same argument implies that there should be a much smaller exchange energy contribution to E_{PSS} in the $[(L)Cr\{CNRu(NH_3)_5\}_n]^{(3+n)+}$ complexes than in the $[Ru(Am)_{6-2n}(bpy)_n]^{2+}$ complexes, and that the light absorption process involves a very large loss of exchange energy in the former but not the latter. Therefore, the electronic state assignments in Figure 12 nicely account for the higher energy MMCT absorptions of the $[(L)Cr\{CNRu(NH_3)_5\}_n]^{(3+n)+}$ complexes, and of the higher energy emission of the $[(bpy)_2Cr\{CNRu(NH_3)_5\}_n]^{5+}$ complex, than would be expected on the basis of the patterns found for the $[Ru(Am)_{6-2n}(bpy)_n]^2$ complexes in Figures 10 and 11.

Since the $[Cr(NH_3)_6]^{2+}$ ground-state has a quintet spin multiplicity ($e_gt_{2g}^3$ in O_h or (a_{1g} or b_{1g})$b_{2g}e_g^2$ in the Jahn−Teller-distorted D_{4h} symmetry), the assignment of a $^2A_1$-$[Cr^{II}(b_2e^3),Ru^{III}(e^3)]$ configuration to the lowest energy excited states is more equivocal for the $[(NH_3)_5Cr\{CNRu(NH_3)_5\}]^{4+}$ and *trans*-$[(NH_3)_4Ru\{NCCr(NH_3)_5\}_2]^{5+}$ complexes than for any of the others of this series. However, $^5Cr^{II}$ species are greatly distorted and one would expect much broader and more intense vibronic sidebands if the emitting state had such a configuration and one would not expect the absorption and emission to correlate with those of the other complexes as well as in Figure 10. Electronic assignments as in Figure 12 seem most consistent with these observations, but a $^5Cr^{II}$ configuration in the emitting species cannot be entirely excluded if only because the emission spectra of these complexes are overall the broadest and hardest to fit of any of this series.

C. Excited State Lifetimes. 1. General Information. Several lifetime-related issues are raised by studies of the Cr(CN)Ru complexes: (a) the high energy emission component that is interpreted as $^2Cr^{III}$-like has a longer lifetime and smaller k_H/k_D isotope effect than the MMCT component, but its lifetime is much shorter than that of the $(^2E)Cr^{III}$ excited state generated from the $[(L)Cr\{CN\}_n]^{(3-n)+}$ parent (Table S7 in the Supporting Information);[12,68] (b) the k_H/k_D isotope effects for the MMCT components are unusually large (Tables 2 and Supporting Information S7);[12,22,23,68] (c) most of the MMCT excited states have ~1 μs lifetimes at 77 K; (d) based on its very weak emission, the MMCT excited state of $[(bpy)_2Cr\{CN-$

$Ru(NH_3)_5\}_2]^{5+}$ appears to have a much shorter lifetime. The first of these issues is reasonably consistent with expectation based on the double minimum model for the lowest energy adiabatic excited state discussed in the preceding section; note that we have not found any Cr(CN)Ru system, or any excitation regime that can be used to obtain only the high energy emission component, and the much shorter lifetime of this component in the Cr(CN)Ru complexes than in the $[(L)Cr\{CN\}_n]^{(3-n)+}$ parent is consistent with a very small barrier or a weak symmetry prohibition for the crossing to the lower energy minimum of the "mixed valence" excited-state PE surface.

2. Implications for High Energy Electron Transfer Processes in the Marcus Inverted Region. It is convenient to use a semiclassical representation of k_{et} (see eq 3),[75]

$$k_{et} = k_{el} k_{nu} \nu_{nu} \tag{10}$$

in which the vibrational modes, $h\nu_{hf}$, that contribute most effectively to electron transfer in the Marcus inverted region enter as combinations of the first order normal vibrational modes ($\nu_{hf} = [n_a\nu_a + n_b\nu_b + n_c\nu_c + ...]$) and when the ν_{hf} are harmonics of a single first order vibrational mode, ν_k,[24]

$$(\kappa_{nu})_k \approx \sum_j \left[\frac{1}{j!}\left(\frac{\lambda_k}{h\nu_k}\right)^j\right][e^{-\{G_k^2/4RT\lambda_s\}}] \tag{11}$$

$$G_k \approx E_{eg}^{0'0} - \lambda_s - jh\nu_k$$

Then, in the weak electronic coupling (H_{eg} small) and single vibrational mode limits[17,24,27,28,75,76]

$$(k_{et})_k \approx \frac{2\pi^2}{h}\frac{H_{eg}^2}{(\pi\lambda_s k_B T)^{1/2}}\sum_j \left[\frac{1}{j!}\left(\frac{\lambda_k}{h\nu_k}\right)^j\right][e^{-\{G_k^2/4RT\lambda_s\}}] \tag{12}$$

At 77 K the exponential factors in eqs 11 and 12 have the properties of a delta function so that the effective relaxation channels are those with $E^{0'0} \approx \sum_k n_k h\nu_k$ (with $\lambda_s \approx 0$ at 77 K). For $h\nu_k \ll E^{0'0}$ and very small displacements in a single normal mode, eq 12 can be put into the form[24,27,45]

$$k_{et} = Ae^{-\gamma_x \frac{E^{0'0}}{h\nu_{x(\max)}}}, \quad \gamma_x = \ln(E^{0'0}/\lambda_{x(\max)}) - 1 \tag{13}$$

Equation 13 can be used for general, qualitative correlations and comparisons, assuming a single "effective" vibrational mode inferred from the maximum amplitude of the difference spectrum (for λ_x and $h\nu_x$), and such a comparison between some of the Cr(CN)Ru complexes and the $[Ru(Am)_{6-2n}(bpy)_n]^{2+}$ complexes is presented in Figure 13.

The correlation in Figure 13 is based on the premise that local bpy vibrational modes tend to dominate the relaxation channels of the Ru-bpy complexes,[33,46,48,50,77] and it suggests that the high frequency N−H vibrational modes are more important for the Cr(CN)Ru complexes, consistent with their much larger k_H/k_D isotope effects. However, such single mode comparisons are potentially misleading and intrinsically more complicated than implied by eq 13 when the excited-state distortions are in many different vibrational modes of the systems compared. The smaller than expected slope of the correlation line in this figure and a resulting calculated rate constant that is too small by at least a factor of 10^3 for the Cr(CN)Ru complexes are both symptomatic of these problems. When the excited-state distortion is in many vibrational modes and for $E^{0'0} \gg h\nu_k$, the 77 K electron transfer rate constants may be represented as the sum over the different relaxation channels (c),

$$k_{et} \approx A\sum_c \left[\frac{1}{N_c!}\Pi_k\left(\frac{\lambda_k}{h\nu_k}\right)^{n_k}\right]\delta_{E^{0'0},\nu'_c} \tag{14}$$

where $\nu'_c = \sum_k n_k\nu_k$ and $N_c = (n_1 + n_2 + n_3 + n_4 + ...)$. Modeling of the multimode issues using eq 14 and rR parameters reported[30] for $[Ru(NH_4)_4bpy]^{2+}$ indicates the following:[78] (a) There are an enormous number of combinations of vibrational modes $h\nu_{hf}$ that approximate the conditions for this equation, and the most important of these have contributions from three or more first order normal modes (ν_a, etc.) in part because of their very large degeneracies (or the number of different orderings of component modes). (b) The bpy distortion mode at 1481 cm^{-1} contributes to many of the more important relaxation channels. (c) Although their Huang−Rhys parameters are extremely small (∼0.001−0.003),[45,48] the high frequency C−H and N−H vibrational modes probably make appreciable contributions to these relaxation channels, but only in combination with a larger number of contributions from vibrational modes in the medium frequency (1200−2000 cm^{-1}) and some in the low frequency (200−1000 cm^{-1}) ranges. The Huang−Rhys parameters appear to be comparably small for distortions of the Cr(CN)Ru MMCT excited states in the N−H vibrational modes,[22,23] while only the C≡N stretching modes appear to make detectable but relatively small contributions ($S_{CN} <$ ∼0.05)[23] in the medium frequency regime. As a result the number of relaxation channels that involve the medium frequency modes will be orders of magnitude smaller for the Cr(CN)Ru than for the [Ru(L)bpy] complexes, their higher order contributions will tend to be relatively more important, and the former class of complexes will tend to have longer lifetimes since the Huang−Rhys parameters for distortions in the N−H modes are so small.

Finally, these arguments and the scheme in Figure 12 suggest a relatively straightforward account for the surprisingly weak $[(bpy)_2Cr\{CNRu(NH_3)_5\}_n]^{5+}$ emission. Thus, if

(74) Nakamoto, K. *Infrared and Raman Spectra of Inorganic and Coordination Compounds. Part B*; Wiley: New York, 1997.
(75) Newton, M. D.; Sutin, N. *Annu. Rev. Phys. Chem.* **1984**, *35*, 437.
(76) Marcus, R. A.; Sutin, N. *Biochem. Biophys. Acta* **1985**, *811*, 265.
(77) The envelope of reorganizational contributions that arise from distortions in internal bpy vibrational modes has been estimated from Huang-Rhys parameters that are based on the $[Os(bpy)_3]^{2+}$ rR spectrum,[33] attenuated as necessary to allow for the effects of excited state-ground state configurational mixing as described elsewhere.[48] Similar correlations reported previously[46,48,50] were based on the net amplitudes of the vibronic sidebands in the medium frequency regime, these amplitudes contain appreciable and varying contributions from 2nd order contributions in the low frequency vibrational modes[48] and the resulting correlation lines are somewhat different.

(78) We have calculated the contributions of about 100 different vibrational combinations containing $n_{1481}\nu_{1481}$, with $1 \le n_{1481} < 9$, $E^{0'0} = 12{,}493$ $cm^{-1} \approx \pm$ 500 cm^{-1} and the vibronic parameters inferred from the rR spectrum of $[Ru(NH_3)_4bpy]^{2+}$. This gives about 7×10^5 different relaxation channels with a net rate constant contribution of $\sim 5 \times 10^5$ s^{-1} based on eq 12, $2\lambda_s RT(\ln(2))^{1/2} = 900$ cm^{-1} and $A = 10^{13}$ s^{-1}.

the MMCT $[Cr^{II}(b_2e^3),Ru^{III}(e^3)]$ excited states with quartet and doublet spin multiplicities differ little in energy in the diabatic limit, then the relative large energy difference between observed MMCT and the $(^2E)Cr^{III}$ emission of the parent $[(bpy)_2Cr\{CN\}_2]^+$ complex implies a smaller extent of metal centered/MMCT excited state/excited-state configurational mixing and the $^4A[(bpy)_2Cr\{CNRu(NH_3)_5\}_n]^{5+}$ MMCT excited-state energy could be lower than or nearly equal to the energy of the $^2B_1[(bpy)_2Cr\{CNRu(NH_3)_5\}_n]^{5+}$ MMCT excited state. However, the distortions of the $^4A_1[Cr^{II}(b_2e^3),Ru^{III}(e^3)]$ and $^2A_1[Cr^{II}(b_2e^3),Ru^{III}(e^3)]$ excited states would be very similar since their orbital populations are identical, and the resulting bandshapes are probably too similar for us to distinguish. In such a case, spin allowed electron transfer relaxation to the ground-state would dominate the excited-state relaxation, that is, $\kappa_{el} \approx 1$ for the ^{4}MMCT excited state, but $\kappa_{el} \ll 1$ for the ^{2}MMCT excited states.

Conclusions

Irradiations of MMCT absorption bands of $[(L)Cr^{III}\{CNRu^{II}(NH_3)_5\}_n]^{(3+n)+}$ complexes at 77 K generate $[(L)Cr^{II}\{CNRu^{III}(NH_3)_5\}_n]^{(3+n)+}$ electron transfer excited states which emit in the near-infrared spectral region, but the resulting MMCT emission energies are only slightly lower than those of the metal centered $(^2E)Cr^{III}$ emissions of the parent Cr^{III} complexes. As a consequence, the bandshapes of the observed emission spectra are generally functions of the excitation energy with excitations at energies greater than the MMCT absorption resulting in greater contributions from $(^2E)Cr^{III}$-like components. Both the metal-centered and MMCT excited-state components appear to be stabilized by configurational mixing, somewhat analogous to that found in mixed valence ground states, but there are a very large number of different, near in energy electronic excited states in these systems and the lowest energy metal-centered and MMCT electronic excited states may be only very weakly mixed. The lowest energy emission is observed for the $[(bpy)_2Cr\{CNRu(NH_3)_5\}_n]^{5+}$ complex, and this emission is extraordinarily weak most likely because the larger separation of the diabatic $(^2E)Cr^{III}$ and MMCT excited states reduces the amount of configurational mixing so that the ^{2}MMCT excited-state energy is no longer significantly less than that of the ^{4}MMCT excited state; without the spin restriction on back electron transfer, the excited-state lifetime is very short.

Acknowledgment. The authors thank the Office of Basic Energy Sciences of the Department of Energy and the Office of the Vice President for Research at Wayne State University for partial support of this research.

Supporting Information Available: Excitation wavelength dependent emission of the *trans*-[(*ms*-Me_6[14]aneN_4)Cr{(CNRu-$(NH_3)_5\}_2]^{5+}$ complex; effect of cyano-mercuration on the ^{2}E emission of *tran*-$[Cr(^{15}1neN_2)(CN)_2]^+$; comparison of Grams32 fits of $[(NH_3)_5Ru\{CNCr(NH_3)_5\}]^{4+}$ and $[(NH_3)_4Ru\{CNCr(NH_3)_5\}_2]^{6+}$; deconvolution of $[(NH_3)_5Ru\{CNCr(NH_3)_5\}]^{4+}$ and $[(NH_3)_4Ru$-$\{CNCr(NH_3)_5\}_2]^{6+}$ emission spectra; the $[(bpy)_2Cr\{CNRu$-$(NH_3)_5\}_2]^{5+}$ emission; excited state d-orbitals in C_{4v} symmetry; luminescence lifetimes of cyanide-bridged transition metal complexes. This material is available free of charge via the Internet at http://pubs.acs.org.

IC8011266